Ocean Dynamics (2004) 54: 92–106
DOI 10.1007/s10236-003-0088-x

Jens-Olaf Beismann · Bernard Barnier

Variability of the meridional overturning circulation of the North Atlantic: sensitivity to overflows of dense water masses

Received: 4 July 2003 / Accepted: 17 December 2003

Abstract A numerical model of the Atlantic Ocean was used to study the low-frequency variability of meridional transports in the North Atlantic. The model shows a behaviour similar to those used in previous studies, and the temporal variability of certain variables compares favourably to observed time series. By changing the depth and width of the sills between the subpolar North Atlantic and the Nordic Seas, the mean horizontal and overturning circulation as well as some water mass properties are modified significantly. The reaction of meridional oceanic transports to atmospheric forcing fluctuations remains, however, unchanged. The critical role of the surface heat flux retroaction term for the meridional heat transport in stand-alone ocean models is discussed. The experiments underline the role of atmospheric variability for fluctuations of the large-scale ocean circulation on time scales from years to decades, and they support the hypothesis that the mean overturning strength is controlled by the model representation of the density of the overflow water masses.

Keywords Overflows · Decadal variability · Meridional overturning · Ocean/atmosphere interactions · Numerical modelling

Responsible Editor: Dirk Olbers

J.-O. Beismann (✉)
Institut für Meereskunde an der Universität Kiel,
Düsternbrooker Weg 20, 24105 Kiel, Germany
e-mail: jobeismann@web.de

B. Barnier
Laboratoire des Ecoulements Géophysiques et Industriels,
BP 53 X, 38041 Grenoble cedex 9, France

Present address: J.-O. Beismann
NEC High Performance Computing
Europe GmbH, Prinzenallee 11, 40549 Düsseldorf, Germany

1 Introduction

The stability and variability of the meridional overturning circulation (MOC) in the North Atlantic are of interest in climate research for at least two reasons: first, the subpolar North Atlantic and the adjacent Arctic Ocean are important elements in the global conveyor belt circulation because here the only locations of deep-water formation in the Northern Hemisphere can be found. Second, the northeastward advection of warm surface water with the North Atlantic Current (NAC; the upper limb of the MOC in the North Atlantic) and the air–sea interaction over the ocean are responsible for the relatively warm climate of western Europe in comparison to other regions of the globe at the same latitude.

Several recent studies have shown that much of the North Atlantic variability during the past decades is related to the North Atlantic Oscillation (NAO). The NAO is the dominant mode of atmospheric variability over the North Atlantic (e.g. Hurrell 1995). Observational studies have documented its influence on the convective activity (Dickson et al. 1996) and on the T/S properties of the Denmark Strait overflow (Dickson et al. 1999), for example. From coupled climate models, the possibility of an oceanic forcing of the NAO has been derived (Rodwell et al. 1999). Ocean-only models have been used in several studies to investigate the oceanic response to the interannual to interdecadal variability in the atmospheric circulation related to the NAO (e.g. Häkkinen 1999; Eden and Willebrand 2001; Krahmann et al. 2001; Gulev et al. 2003). These mainly coarse-resolution ocean models show instantaneous and delayed responses of both the horizontal and the overturning circulation as a reaction to fluctuations in the atmospheric forcing fluxes.

Numerical ocean models like those used in the studies mentioned above suffer from an unrealistically large diapycnal mixing in regions where dense waters descend topographic slopes (Willebrand et al. 2001). As a result of this, these models usually show a too-shallow

meridional overturning cell because the density of the simulated overflow water masses is too low in comparison to observations. The ocean components of coupled climate models with their even coarser horizontal and vertical resolution are known for their deficiencies in the representation of deep-water formation. Döscher and Redler (1997) argue that the atmospheric influence on the subpolar North Atlantic might be overestimated if the northern overflows are not adequately represented in models. This raises the question of whether results of studies like Eden and Willebrand (2001) or Häkkinen (1999) would change under different overflow conditions.

Roberts and Wood (1997) have shown in a coarse-resolution ocean model the sensitivity of the large-scale circulation to slight changes of topographic details in the Greenland–Iceland–Scotland ridge. With deepened passages, the mean transport of dense water across the ridge and the meridional overturning strength increase significantly. The regions of convection shift from the Iceland Basin into the Norwegian Basin, and the depth of the mixed layers in the subpolar basins is limited by the underlying dense waters. Along with the changes of the overturning, modifications of the meridional heat transport (MHT) of more than 50% are observed in their experiments with deep passages. This would possibly have important impact in coupled climate simulations if the ocean component of a coupled model reacted in a similar way.

Beckmann and Döscher (1997) have proposed a parameterization of the processes in the bottom boundary layer (BBL) that allows dense waters to descend topographic slopes in ocean models without strong diapycnal mixing. Using a simplified BBL parameterization in sensitivity studies with an idealized model of the North Atlantic, Lohmann (1998) shows that the meridional overturning circulation can recover its original strength after a breakdown induced by a large surface freshwater anomaly. Without the BBL, the overturning remains in a reduced state and breaks down completely after several centuries. His study thus supports the findings of Döscher and Redler (1997) concerning the role of the overflows for the sensitivity of the overturning circulation. It is, however, not yet clear whether these conclusions are also true for moderate forcing variations such as the NAO-related variability over the North Atlantic.

The objective of the present study is to investigate the robustness of the simulated response of the MOC in the North Atlantic to atmospheric forcing fluctuations as observed during the past decades under different circulation regimes characterized by different representations of the northern overflows. To this end, the model bathymetry in the region of the Greenland–Iceland–Scotland ridge is modified to allow for stronger overflows of dense water. These sensitivity studies are similar to the experiments by Roberts and Wood (1997), but the emphasis of the analysis is more on the variability of the large-scale circulation and meridional transports and on a possible modification of the atmospheric influence on the ocean.

The paper is organized as follows: in Section 2 we describe the numerical model used in this study. Section 3 shows some elements of the large-scale circulation in a reference experiment and their variability during the period from 1963 to 1997. In Section 4, we compare the mean circulation in experiments with modified northern sills as well as its variability. A discussion of the results concludes this study.

2 Model description and experimental design

The ocean model used in this study is the primitive equation model OPA8.1 (Madec et al. 1998, 1991) with some additional features developed in the CLIPPER project (Tréguier et al. 1999). The model has an isotropic horizontal grid with a resolution of $1^\circ \times 1^\circ \cdot \cos\phi$ (longitude $\times$ latitude). There are 43 geopotential levels in the vertical, with layer thicknesses varying from 12 m at the surface to 200 m below 2000 m depth and a maximum depth of 5500 m (cf. Table 1). The model domain is the Atlantic Ocean from 75°S to 70°N, with rigid walls at the northern and southern boundaries. At these boundaries, as well as at the Strait of Gibraltar, which is closed in this model configuration, restoring zones for potential temperature and salinity are used to represent the influence of the adjacent seas.

The model has open boundaries at Drake Passage and south of Africa (30°E). The open boundary algorithm is a combination of radiation (Orlanski 1976) and relaxation to climatology, based on the numerical scheme implemented by Barnier et al. (1998) in a regional model of the South Atlantic. A barotropic inflow (outflow) of 130 Sv is prescribed at Drake Passage

Table 1 Depth (in m) of the temperature and velocity points

Level number	Depth (m)	Level number	Depth (m)
1	6	23	1610
2	18	24	1806
3	30	25	2003
4	42	26	2202
5	55	27	2401
6	68	28	2600
7	81	29	2800
8	96	30	3000
9	112	31	3200
10	132	32	3400
11	155	33	3600
12	186	34	3800
13	227	35	4000
14	282	36	4200
15	356	37	4400
16	452	38	4600
17	572	39	4800
18	713	40	5000
19	872	41	5200
20	1045	42	5400
21	1228	43	5600
22	1417		

(30°E), whereas climatological data (Reynaud et al. 1998) are used as relaxation data for tracers and baroclinic velocities. Details on the implementation of open boundaries in OPA8.1 are given in Tréguier et al. (2001).

The model employs isopycnal diffusion and Laplacian lateral friction to parameterize the mixing effect of mesoscale eddies. The values of the coefficients are $2.5 \times 10^3\ m^2\ s^{-1}$ (diffusivity) and $5 \times 10^3\ m^2\ s^{-1}$ (viscosity) at the Equator, and they decrease with the cosine of the latitude. Vertical diffusivity and viscosity coefficients are calculated at each time step by a turbulent kinetic energy model implemented by Blanke and Delecluse (1993) with minimum values varying from $10^{-4}\ m^2\ s^{-1}$ at the surface to $10^{-5}\ m^2\ s^{-1}$ below 48 m. An enhanced vertical diffusivity of $1\ m^2\ s^{-1}$ is used to account for the effects of convection if the density profile becomes unstable.

Monthly mean surface-flux data for the period 1958 to 1997 from the NCEP/NCAR reanalysis project (Kalnay et al. 1996) were used to force the ocean model. To achieve a quasi-equilibrium state, the model was forced for 70 years by climatological monthly means of the above-mentioned 40-year period. Fluxes of heat and freshwater as well as wind stresses were applied as boundary conditions at the surface layer in the formulation given by Barnier (1998). Solar shortwave fluxes are treated separately, thereby allowing them to penetrate to and distribute their effect over deeper model layers. A restoring term (as given by Barnier et al. 1995) to the NCEP sea-surface temperature was added to the total heat flux. A motivation for this term and its description are presented in the Appendix. The restoring time scale included a seasonal and geographical dependence to take into account the retroaction of the sea-surface temperature on the heat flux. A typical value for the restoring time scale is 14 days (for a surface layer of 12 m depth). With the same time scale, a restoring of the surface salinity to a seasonal climatological value (taken from the climatology by Reynaud et al. 1998) was added as a correction to the freshwater flux.

A simple representation of the effects of sea ice was incorporated by using a so-called zero-order ice model: if the NCEP SST is below the freezing point calculated from the model SSS, heat and freshwater fluxes are set to zero and a strong restoring (time scale 3 days) to the freezing temperature and a climatological SSS (Reynaud et al. 1998) is introduced.

Three experiments with interannually varying surface forcing have been carried out. The first experiment (NCEP1) is described in Section 3, while Section 4 gives a comparative analysis of NCEP1 and the other two experiments (NCEP2, NCEP3). Each of the three experiments has a different topography in the region of the Greenland–Iceland–Scotland (GIS) ridge: NCEP1 started with a topography obtained from a global dataset (Smith and Sandwell 1997) by standard interpolation methods. The overflows of dense water being rather weak in this experiment, we slightly deepened the Denmark Strait and introduced a deep wide connection from the Norwegian Sea to the North Atlantic between the Faeroe Islands and Scotland in NCEP2 (Fig. 1). In NCEP3, we tried to represent more realistically the complex topography of the Faeroe Bank Channel (Fig. 1). After a spinup with their respective

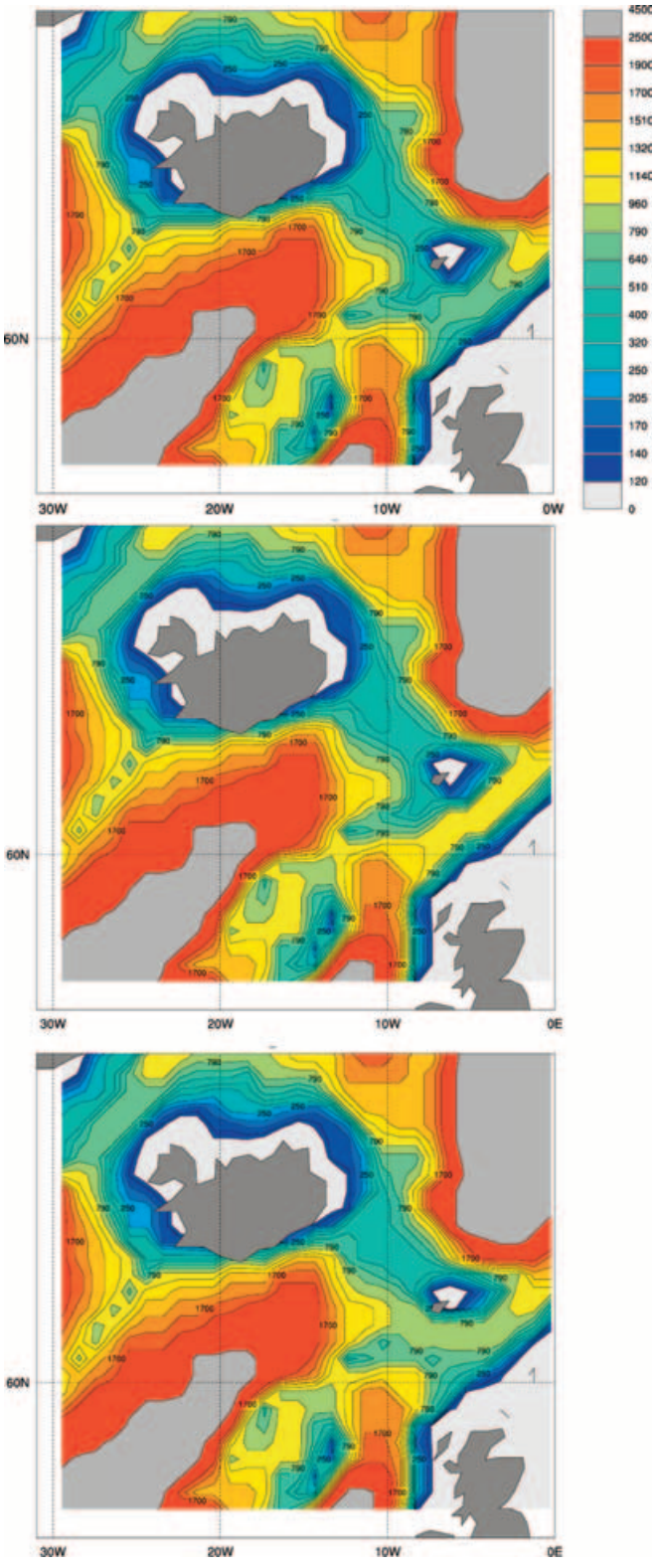

Fig. 1 Bathymetry (in m) in the region of the Greenland–Iceland–Scotland Ridge. *Top* NCEP1; *middle* NCEP2; *lower* NCEP3

topography, all experiments were integrated for the period from 1958 to 1997 using the same surface forcing.

3 Mean circulation and interannual variability

3.1 Mean circulation state after the spinup

In order to evaluate the model performance, we start with a brief analysis of the mean circulation after the spinup. The vertically integrated circulation after the spinup (Fig. 2) is typical for state-of-the-art z-coordinate ocean models of comparable resolution (e.g. Eden and Willebrand 2001; Gulev et al. 2003). The strength of the subpolar gyre in the North Atlantic is higher than 20 Sv, whereas the subtropical gyre has a maximum strength of 38 Sv, which is consistent with observations by Schott et al. (1988). As in most coarse-resolution models, the separation point of the Gulf Stream is situated too far north in our simulation. In the South Atlantic the circulation is dominated by zonal currents associated with the frontal systems. The transport of the Antarctic Circumpolar Current (ACC) is prescribed to 130 Sv at the open boundaries. Directly after entering the model domain at Drake Passage, the ACC splits into two branches, the northern of which follows the continental shelf to the north and forms the confluence with the Brazil Current off the Argentine coast. The confluence zone is located between 45° and 50°N, which is farther south than observed (Peterson and Stramma, 1991). In the eastern basin, the Agulhas current enters the model domain at the southern tip of Africa. Part of it retroflects at about 20°E, while most of the flow continues toward the northwest. A second retroflection point is located at the Greenwich meridian.

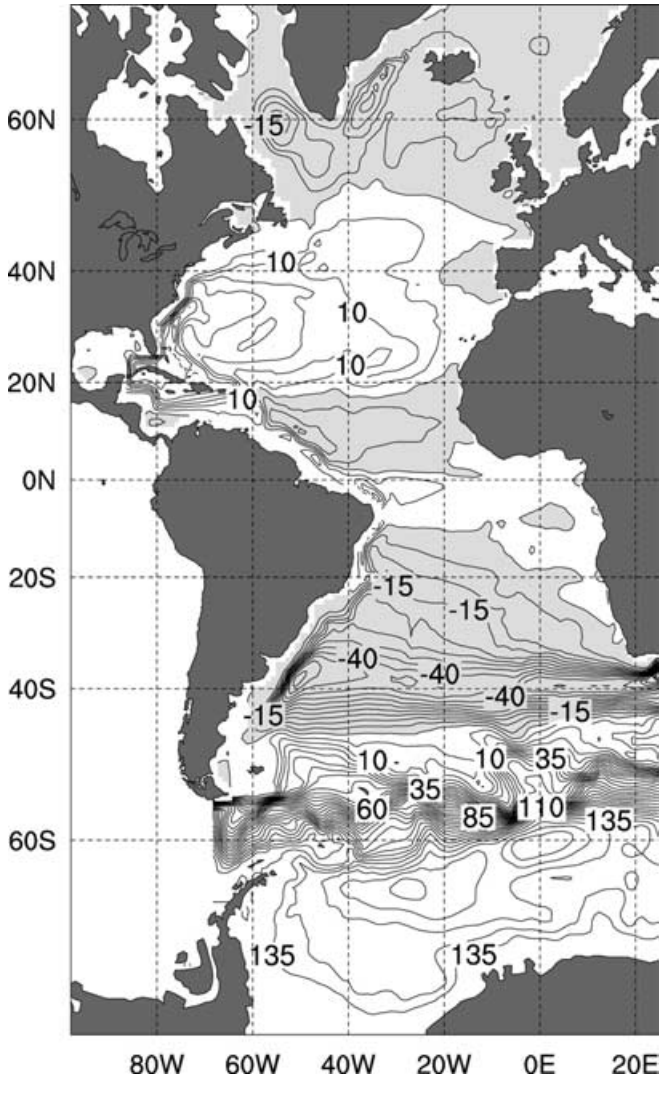

Fig. 2 Barotropic streamfunction (in Sv; contour interval 5 Sv). *Shaded areas* indicate negative values (counterclockwise flow). Annual mean of year 70 for the spinup

Figure 3 shows the vertical structure of the meridional overturning cell after the spinup phase. The maximum transport is 16 Sv, distributed over the region between 25°N and 45°N at a depth of 800–1000 m. Three Sv of water of nordic origin cross the northern sills at 64°N and enter the subpolar Atlantic. The southward transport of deep water increases rapidly between 65°N and 60°N, indicating that most of the transformation of surface and mode water to North Atlantic Deep Water (NADW) in this model takes place south of the sills. Between 14 and 15 Sv of NADW cross the Equator on their way south, with the transport being distributed over the depth range between 1200 and 3500 m. The shape and the strength of the overturning cell in the North Atlantic are consistent with other North Atlantic models (Döscher and Redler 1997; Willebrand et al. 2001).The overturning stream function did not show any significant temporal trend during the last decades of the spinup.

The MHT (Fig. 4) as a function of latitude has a maximum value of 0.97 PW at 17°N (1 PW = 10^{15} W), which is in the lower range of the estimate given by Macdonald and Wunsch (1996) (see also the more recent estimates by Ganachaud and Wunsch 2003 and Talley 2003). The absolute values and the shape of the heat-transport curve, however, compare favourably with results given by other numerical ocean models (Böning and Bryan 1996). This section thus shows that our reference experiment started from a reliable and, in many aspects, realistic circulation state.

3.2 Interannual variability

NCEP1 started in 1958. We will, however, restrict our analysis to the period from 1963 to 1997 since the first 5 years of this experiment were characterized by adjustment processes transmitted by waves that had been excited by the switch from climatological to interannually varying forcing. Inspection of basin-wide integrated temperature (not shown) shows that this is long enough for the adjustment oscillations to decay.

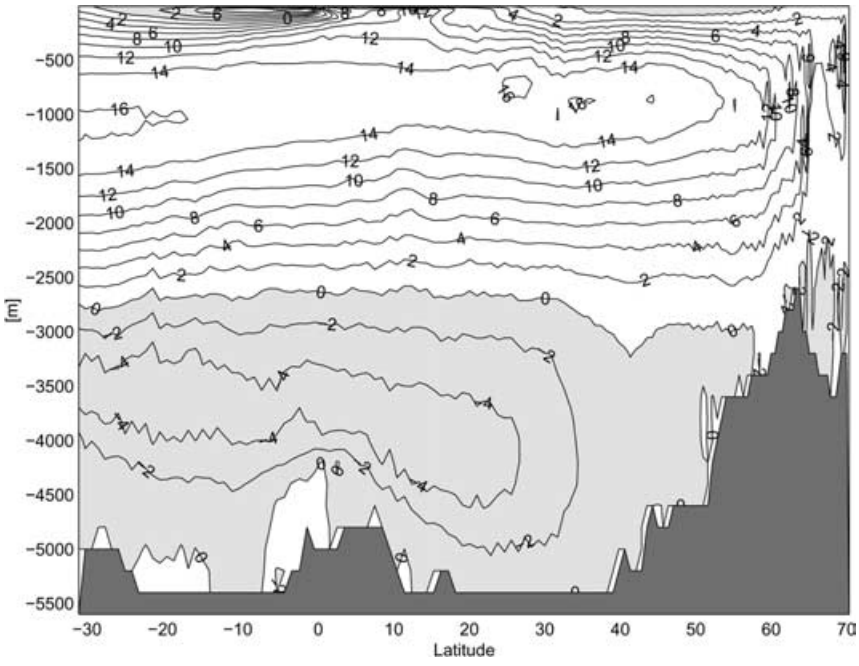

Fig. 3 Streamfunction (in Sv; contour interval 2 Sv) of the zonally integrated flow; annual mean of year 70 for the spinup. *Shaded areas* indicate negative values (counterclockwise flow)

When forced by interannually varying atmosphere–ocean fluxes, the maximum of the overturning streamfunction at 48°N shows considerable variability on interannual to interdecadal time scales (Fig. 5). Deviations from the mean value over the period 1963–1997 can be as high as 15.2% of the mean value. Superimposed on the strong interannual fluctuations is a linear enhancement trend of about 0.05 Sva^{-1}. Also shown in Fig. 5 is the corresponding time series from a simulation with the model used by Eden and Willebrand (2001). Although the mean value of the overturning at 48°N is slightly higher in this experiment, the phase and amplitude of the fluctuations is very similar to our case NCEP1, indicating that our model reacts in a very similar way to interannual variability in the forcing fluxes.

The mechanisms of the modelled oceanic response to fluctuations in the atmospheric forcing have been described by Eden and Willebrand (2001) and Gulev et al. (2003). They have shown that the meridional overturning reacts with a delayed enhancement (time lag 2–3 years) to anomalous deep convection in the Labrador Sea (caused by anomalous oceanic heat losses during phases of high NAO), combined with a spinup of the cyclonic subpolar gyre circulation. Superimposed on this is an instantaneous response to fluctuations in the wind-stress forcing associated with changes in the Ekman transport. The delayed reaction

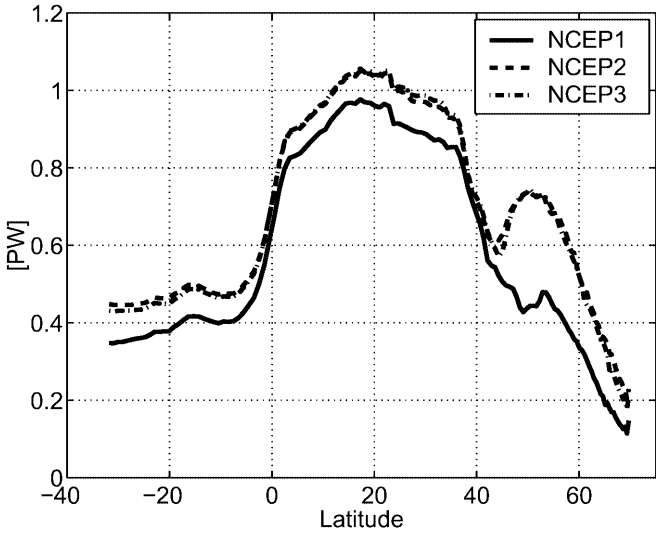

Fig. 4 Meridional heat transport (in PW, 1 PW = 10^{15} W) in experiments NCEPl, NCEP2, and NCEP3. Mean values over the period 1988–1997

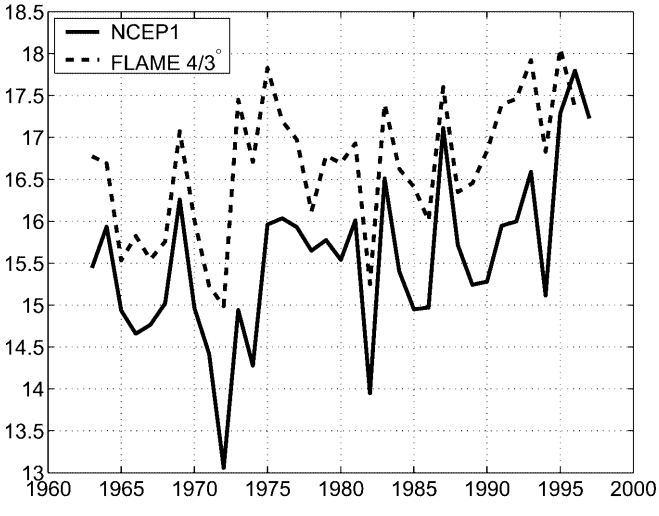

Fig. 5 Time series of the maximum value of the overturning streamfunction at 48°N (annual means, in Sv) from experiment NCEP1 and a simulation with the FLAME model used by Eden and Willebrand (2001)

to wind-stress changes consists in an enhancement of both the subtropical and subpolar gyre circulation. Since both our model configuration and the atmospheric forcing fluxes are very similar to their study, the reader is deferred to Eden and Willebrand (2001) for a detailed discussion of these mechanisms.

The long-term enhancement trend in the meridional transport in NCEP1 is governed by the enhancement of the NAO over the past four decades, as demonstrated in similar model studies (e.g. Eden and Willebrand 2001; Krahmann et al. 2001; Gulev et al. 2003). Interannual fluctuations in the zonal wind stress τ_x induce strong year-to-year changes in the overturning in higher latitudes (cf. Fig. 5). These changes are brought about by an instantaneous reaction to modifications in the surface Ekman transport. To demonstrate how our model reacts to fluctuations in the surface heat flux, Fig. 6 shows the mean temperature of Labrador Sea Water (LSW) in its formation region. The simulated changes in the LSW temperature characteristics are in close agreement with observations (with caution for the period 1975–1983 due to the scarcity of observational data). One exception is the cooling trend between 1988 and 1995. The resultant temperature drop was underestimated by our model. This underestimation could be caused by an inaccurate representation of the interannual variability of the freshwater fluxes in the NCEP/NCAR data and the use of climatological data for SSS relaxation, or by a misrepresentation of non-linear processes due to the coarse model resolution. However, the periods of strong convection (1972–76, 1982–85, 1988–92) are reflected by cooling of the LSW. Comparison with Fig. 5 shows that the meridional transport increases in the years after strong convection and reaches maximum values approximately 3 years after the onset of convection, in a manner similar to that described by Eden and Willebrand (2001).

In order to make the link between convection and formation of LSW on the one hand and the meridional transport on the other hand clearer, Fig. 7 shows a time series of the rate of winterly dense-water formation in the Labrador Sea. The correlation to the overturning time series at 48°N is 0.62 when the dense-water formation leads by 2 years, and 0.7 when the dense-water formation leads by 3 years. The results of this section thus corroborate the findings of Eden and Willebrand (2001). The interannual fluctuations in our simulation compare favourably with observations (given the limitations imposed by model resolution and setup), and – because of the strong similarity of the models – are caused by the same mechanisms as described by Eden and Willebrand (2001).

4 Sensitivity to representation of northern sills

4.1 Mean circulation

In this section, long-term means over the years 1988 to 1997 of each of the three experiments are used to identify the differences induced by the changes in the representation of the northern sills.

Döscher and Redler (1997) found that the overturning strength is governed by the representation of the overflow water masses in their model of the North Atlantic, which has its northern boundary at 65°N and thus does not explicitly include the overflow processes. The transport of dense water through Denmark Strait was rather realistic in our simulation NCEP1 (3.7 Sv, as compared to a transport of 3.8 ± 0.8 Sv of cold water as observed by Girton et al. 2001), but only 1.5 Sv passed through the sills between Iceland and Scotland.

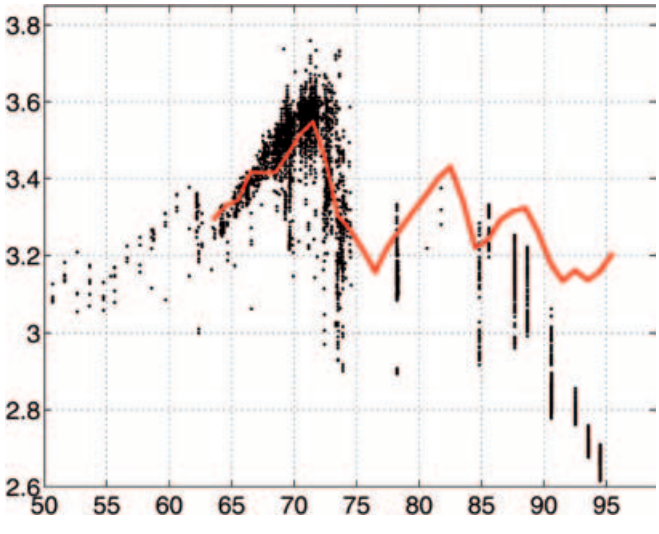

Fig. 6 Annual mean temperature at 1500 m in the Labrador Sea from experiment NCEPl (*red line*). Also shown are temperature data between 1300 and 1800 m from within a circular region of 300 km diameter around Ocean Weather Ship *Bravo* (Yashayaev 2001)

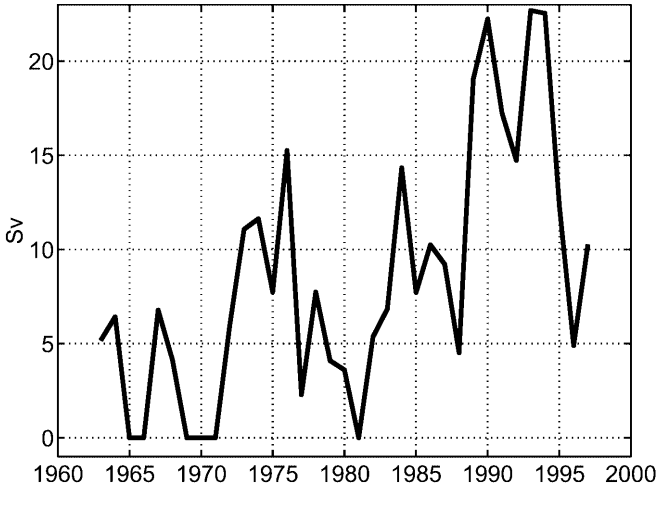

Fig. 7 Time series of deep-water formation rates, defined by the volume of newly formed dense water ($\sigma_0 > 27.75$) in the Labrador Sea between 50°N and 65°N. The calculation of the formation rate is based on the difference in dense-water volume between the end of March and the middle of the preceding December for each year

Directly south of the sills, the dense water was rapidly being mixed with lighter ambient water which led to an underestimation of the maximum density that could be found in the Irminger Basin in NCEP 1 (cf. Fig. 8). This behaviour is common for many ocean models, especially for those using a step-wise representation of bottom topography (e.g. Willebrand et al. 2001).

Figure 9 shows a number of dramatic changes in the horizontal circulation between experiment NCEP1 on the one hand and NCEP2 and NCEP3 on the other. Over the whole width of the basin, the cyclonic circulation of the subpolar gyre extends farther south in the case with a deepened Faroe Bank Channel. The Gulf Stream transport in NCEP2 is about 10 Sv higher than in NCEP1, and the axis of the North Atlantic Current (NAC) has turned from the northeasterly path into the Irminger Basin to a zonal direction until it reaches the Mid-Atlantic Ridge at 32°W. In the Iceland and Irminger Basins the circulation along topographic contours has increased in strength, indicating that more ISOW (Iceland–Scotland Overflow Water) passes from the Iceland–Scotland ridge into the subpolar gyre. The vertically integrated transport in the Labrador Sea does not differ very much between NCEP1 and NCEP2. The meridional overturning is stronger in NCEP2; at 48°N the overturning cell has increased by 1.5–2 Sv (Fig. 13).

These changes in the barotropic circulation can be explained with the JEBAR concept (Sarkisyan and Ivanov 1971). In comparison to NCEP1, the cold and dense water that passes through the Iceland–Scotland ridge in NCEP2 creates a temperature anomaly on the slopes. This change in the stratification produces a cyclonic circulation anomaly that enhances the subpolar gyre in this region, thereby pushing the path of the NAG to the southeast. Penduff et al. (2000) observe very similar modifications of the subpolar gyre in their experiments with a regional model of the northeast Atlantic ocean.

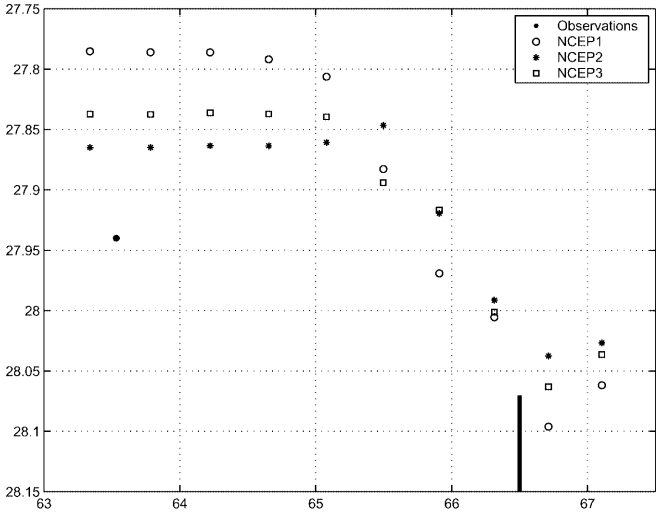

Fig. 8 Maximum of the potential density σ_0 as a function of latitude close to the sills between the subpolar gyre and the Nordic Seas. Observations are a compilation of cruise data sampled between 1996 and 1999 (Käse et al. 2003). The latitude of Denmark Strait is marked by the *thick line*

The change in the path of the NAC causes more North Atlantic water to flow over the Iceland–Scotland ridge into the GIN sea. In NCEP2 and NCEP3 the transformation from surface water into dense deep waters therefore mainly takes place north of Iceland, whereas an unrealistically large downwelling in the Irminger Basin could be observed in NCEP1. In return, the flow of deep water through the passages and into the North Atlantic has to increase, since our model domain is closed at 70°N. In NCEP1, approximately 5.2 Sv of dense water crossed the Greenland–Iceland–Scotland ridge, a value that is at the lower bound of the observed range of transports (Hansen and Østerhus 2000; Girton et al. 2001). The deep passage between Scotland and the Faroes causes an increase of 6 Sv in the ISOW transport (cf. Fig. 9), while the mean transport through Denmark Strait does not change. In NCEP3 the mean ISOW transport is approximately 4.3 Sv (2.8 Sv higher than in NCEP1), and the transport through Denmark Strait is 5.7 Sv. Due to the coarse representation of the narrow sills, the transport of dense water is overestimated in both experiment NCEP2 (11.2 Sv) and NCEP3 (10 Sv), but it is interesting to see how the different depths and widths of the passages affect the partitioning of the total transport between Denmark Strait and the gaps southeast of Iceland.

In spite of the large increase in the transport of dense water, the density of DSOW (Denmark Strait Overflow Water) in the Irminger Basin is still significantly lower than observed (Fig. 8). The maximum density in NCEP2 and NCEP3 lies between 27.84 and 27.86, in comparison to observed values of 27.94–27.95. Once again, this shows that z-coordinate models overestimate the diapycnal mixing with ambient waters due to the stepwise representation of the bottom slopes. Parameterizations of the processes in the bottom boundary layer could remedy this deficiency (e.g. Döscher and Beckmam 2000).

Figure 10 shows the structure of the deep currents in the three experiments. In NCEP1 a clearly defined Deep Western Boundary Current (DWBC) exports NADW from the subpolar gyre to the south. The DWBC, however, is mainly fed by a current that has its origin in the Irminger Basin and follows the western flank of the Reykjanes Ridge into the Newfoundland Basin. This is a questionable feature of this simulation, since this current short circuits the observed cyclonic DWBC path through the Irminger and Labrador Seas as described by, e.g. McCartney (1992). In the eastern basins, no significant transport can be found in NCEP1.

The stronger overflows over the Iceland–Scotland ridge change this picture in experiments NCEP2 and NCEP3. In both simulations ISOW follows the eastern flank of the Reykjanes Ridge to the latitude of the Charlie Gibbs Fracture Zone (CGFZ), where a small

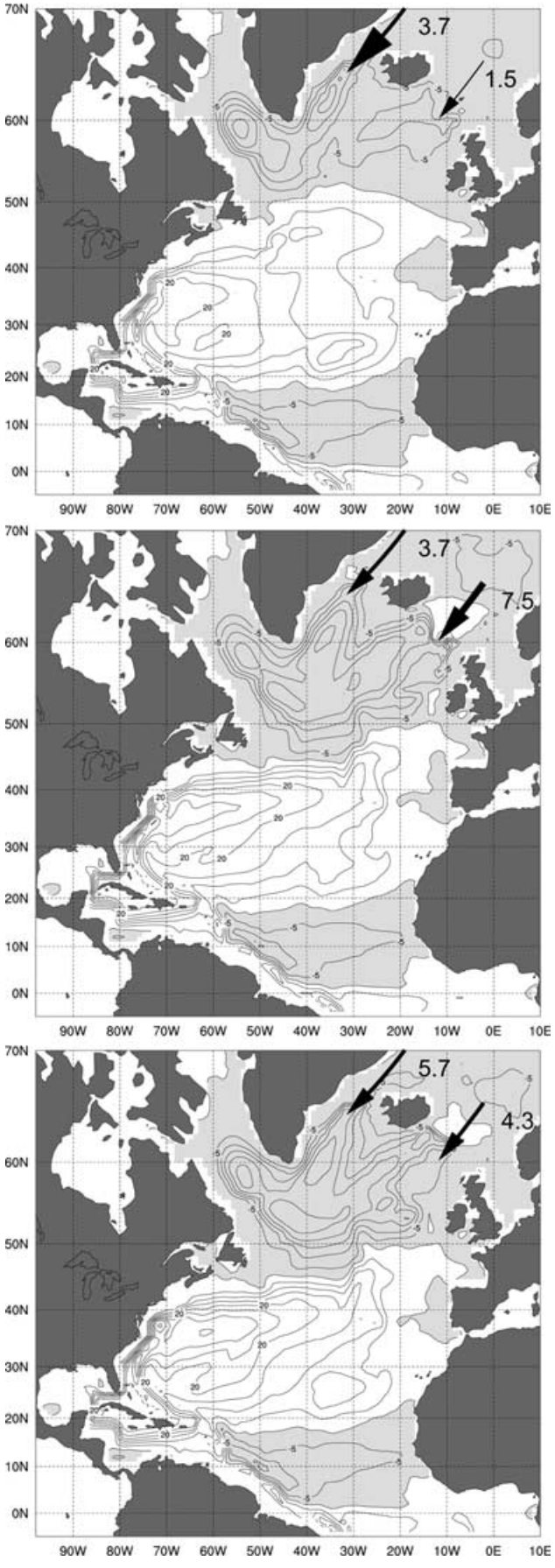

Fig. 9 Barotropic stream function in experiments NCEPl, NCEP2 and NCEP3 (contour interval 5 Sv). To the west and east of Iceland, *arrows together with transport numbers* (in Sv) indicate the strength of the transport of dense water into the subpolar North Atlantic

fraction turns west and flows along the ridge and into the Irminger Sea. Most of the ISOW, however, takes an eastward path through the Porcupine abyssal plain and flows south as a western boundary current on the eastern flank of the Mid-Atlantic Ridge (MAR). In NCEP2, some overflow water reaches the Porcupine abyssal plain via a direct path through Rockall Trough, whereas in NCEP3 the dense waters take a route along both sides of the Iceland Basin. In the Irminger Basin the deep flow is entirely cyclonic in both NCEP2 and NCEP3, and the south-westward flow along Reykjanes Ridge into the Newfoundland Basin does not occur as it did in NCEP1.

In the western basin, the DWBC does not follow the American continental slope around the Grand Banks of Newfoundland, but it makes a sharp turn to the east at 50°N until it reaches the MAR. Some dense waters pass through CGFZ and rejoin with the southward flow in the eastern basin, while most of the DWBC follows the MAR to a latitude between 38 and 42°N, where it turns to the west again. Approximately 5–8° further south the deep flow from the eastern basin turns to the west and crosses the MAR. It rejoins the western part of the deep flow, and a clearly defined DBWC is reestablished on the continental slope between 20°N and 25°N. This deep flow pattern is very similar to that described by Beismann and Redler (2003) in their analysis of tracer simulations with a non-eddy-resolving model. Our experiments suggest that two modes of deep circulation might exist in the subpolar North Atlantic and that the relative strength of the overflows to west and east of Iceland controls in which state the circulation is (this is further discussed in Sect. 5). Although the absence of a DWBC in experiments NCEP2 and NCEP3 is not realistic, the possibility of the existence of additional interior NADW export pathways deserves further study with high-resolution models, which is beyond the scope of this study.

The MHT shows some interesting differences between the experiments. As shown in Fig. 4, the MHT as a function of latitude is higher in NCEP2 than in NCEP1. In the subtropics the stronger northward heat transport can be explained by the fact that it is very closely related to the strength of the meridional overturning at these latitudes (Böning et al. 2001). North of 40°N–45°N, however, the changes in the horizontal circulation pattern affect the mean MHT strongly. A comparison of the net surface heat fluxes of the two experiments with the NCEP/NCAR forcing fluxes explains this effect: in NCEP1 much of the large-scale structure of the forcing fluxes (Fig. 11a) is preserved in the net heat flux as seen by the ocean model, i.e. including the relaxation term towards the climatological SST (Fig. 11b). In NCEP2, however, the modified NAC path allows the cold surface waters from the subpolar gyre to reach farther south

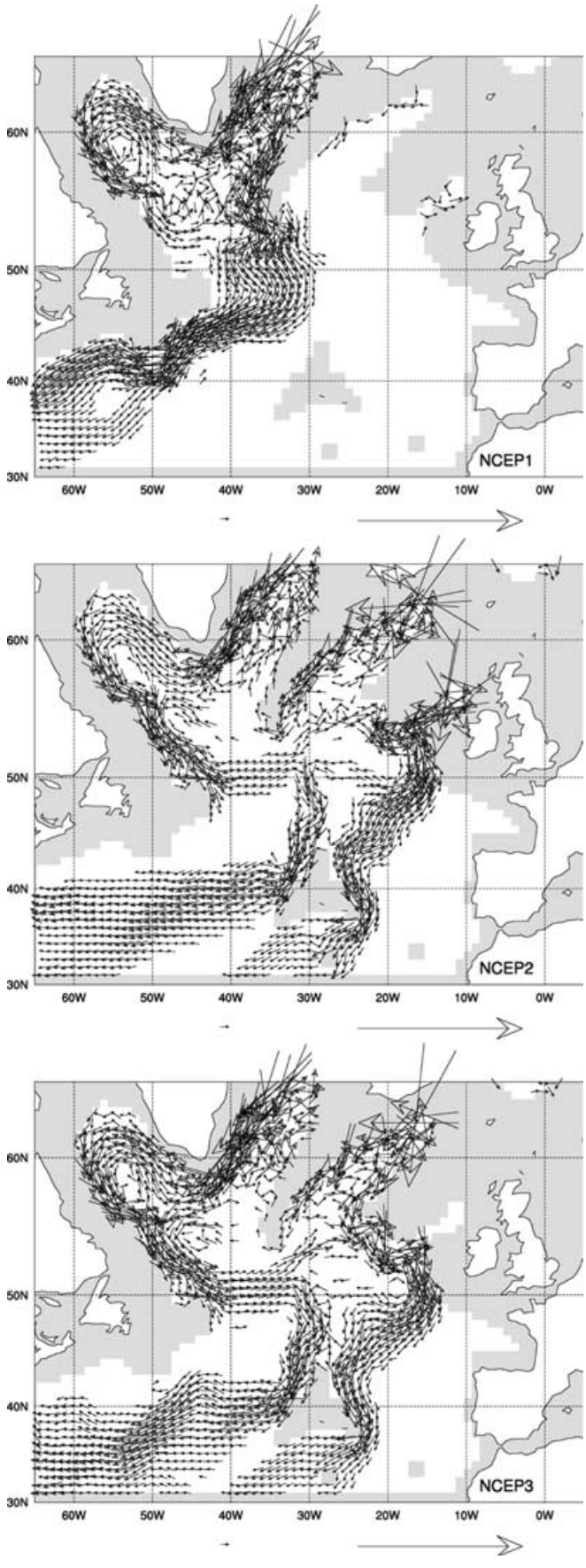

Fig. 10 Deep currents (2000 m) in experiments NCEPl, NCEP2 and NCEP3. Maximum vector: 12 $cm^{-1}s$; minimum vector: 0.5 $cm^{-1}s$. *Shaded areas*: topography

than in NCEP1, which – via the retroaction surface heat flux – turns the region between 45°W and 30°W and 43°N and 53°N from a net cooling region to a region of oceanic heat gain (Fig. 11c). In large parts of this region the retroaction term exceeds values of 200 Wm^{-2} in the long-term mean, leading to an increase of the MHT from 0.6 PW at 45°N to 0.74 PW at 50°N (Fig. 4).

4.2 Interannual variability

We now examine whether the different representation of the overflow water masses has an influence on the sensitivity of the oceanic circulation to atmospheric forcing fluctuations, as discussed in Section 3.

As described in the previous section, the mean transport of dense overflow waters (DSOW/ISOW) over the northern sills changes when the deep passages are modified. The ISOW transport shows little interannual fluctuations in all three experiments, as also the DSOW transport in NCEP1. With the Denmark Strait deepened, however, the flow through this passage shows considerable interannual variability and a weak tendency to stronger transports from the early 1960s to the 1990s. The range of DSOW transports is between 3 and 4.2 Sv in NCEP2 and between 5.2 and 6.2 Sv in NCEP3. This enhanced overflow variability can be interpreted as a response to the modified NAC path: with the NAC carrying more North Atlantic water into the GIN sea, the outflow of DSOW into the subpolar basin has to react to NAC transport fluctuations (induced by atmospheric fluctuations over the subpolar North Atlantic) because our model domain is closed at 70°N. In NCEP1, on the other hand, NAC fluctuations mainly ended up in the Irminger Sea and therefore had no repercussions on the Denmark Strait overflow. In none of the experiments could a significant correlation between the fluctuations of the transport of dense water across the sills and the variability of the overturning at 48°N be established (even with time lags), which underlines the fact that only the mean overturning strength is affected by changing the overflow representation.

As in the previous section, we will use the mean temperature of LSW at 1500 m depth as a measure of the convective activity in Labrador Sea. This will provide insight into the sensitivity of a local process that is governed by the variability of air-sea fluxes to the changed mean circulation state. Figure 12 shows that the mean LSW temperature is higher by about 0.5 °C in both experiments NCEP2 and NCEP3. This is due to the change in the NAC path that does not flow northwestward through the Newfoundland Basin and does not have a Northwest Corner in these simulations. Because of the way the model is forced, the retroaction term in

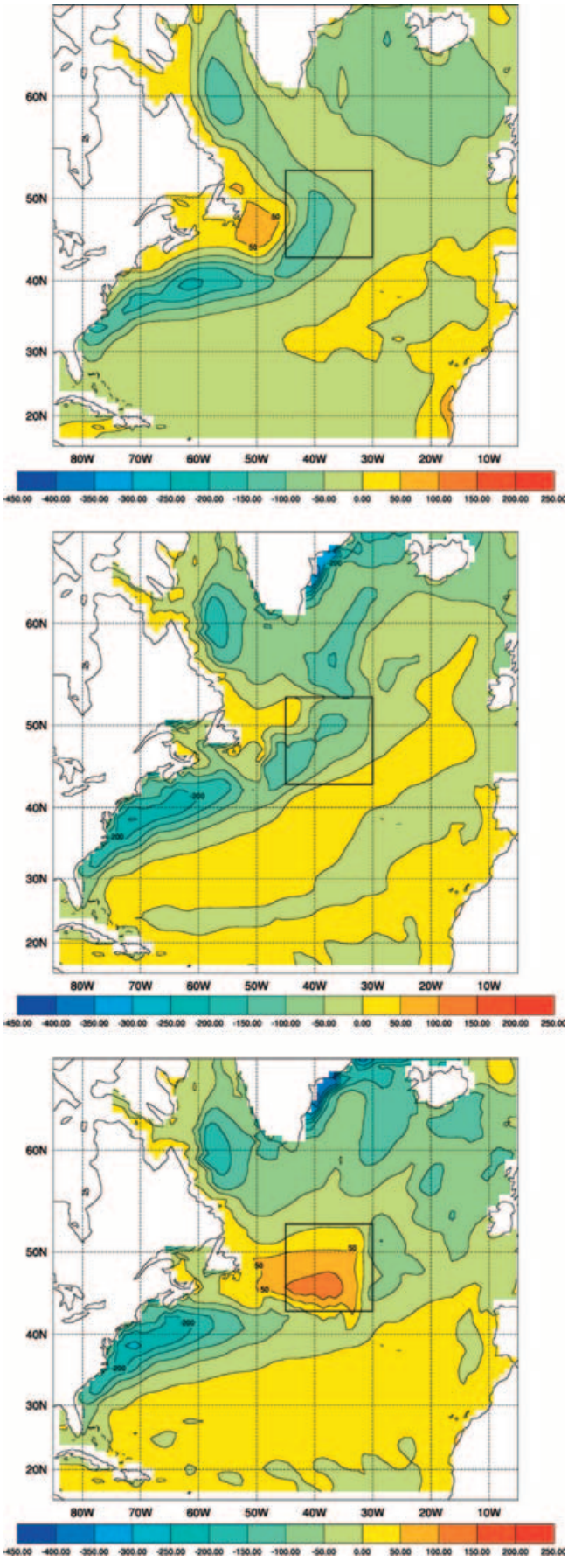

Fig. 11 Net surface heat flux (Wm^{-2}, mean 1988–1997). *Top* NCEP/NCAR reanalysis data; *middle* experiment NCEP1; *bottom* experiment NCEP2. Figures from our experiments include the effect of the SST retroaction term. The *box* indicates the region discussed at the end of Section 4.1

Fig. 12 Time series of the mean temperature at 1500 m in the Labrador Sea in NCEP1, NCEP2 and NCEP3

the heat flux acts as permanent source of heat in these regions, which is the reason for the higher than observed LSW temperature. The periods of LSW cooling and heating, however, remain the same as in NCEP1. The amplitudes of the temperature fluctuations in experiments NCEP2 and NCEP3 are comparable to those in NCEP1. This indicates that the atmospheric influence on the interannual variability of Labrador Sea convection remains the same under the changed circulation regimes.

As a second example, we compare the overturning in the three experiments to see whether the large-scale variability in the North Atlantic is still significantly influenced by atmospheric fluctuations. We have described in Section 3 how the interannual variability in the atmospheric forcing fluxes affects the meridional overturning either directly or indirectly, e.g. via modification of the intensity of winter convection in the Labrador Sea. Figure 13 shows time series of the overturning stream function at 48°N from all three experiments. As has been noted before, the mean overturning is approximately 2 Sv stronger in experiments NCEP2 and NCEP3 than in NCEPl; but the year-to-year changes and the long-term trend of enhancement during the late 1980s and the 1990s remain almost unaffected by the modifications of the mean circulation state. Each peak in the NCEP1 time series can also be found in the other two time series, and it is only the amplitude of the fluctuations that changes slightly in the experiments with stronger overflows.

The important modifications of the mean MHT between experiments NCEP1 and NCEP2 raise the question whether the surface heat-flux retroaction term

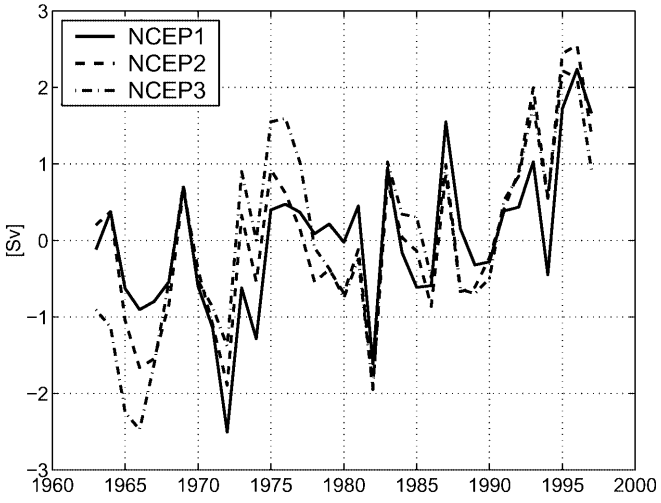

Fig. 13 Anomalies of the maximum of the overturning streamfunction (in Sv) at 48°N in NCEPl, NCEP2 and NCEP3. The following mean values have been subtracted from the time series: NCEPl – 15.56 Sv, NCEP2 – 17.67 Sv, NCEP3 –18.06 Sv

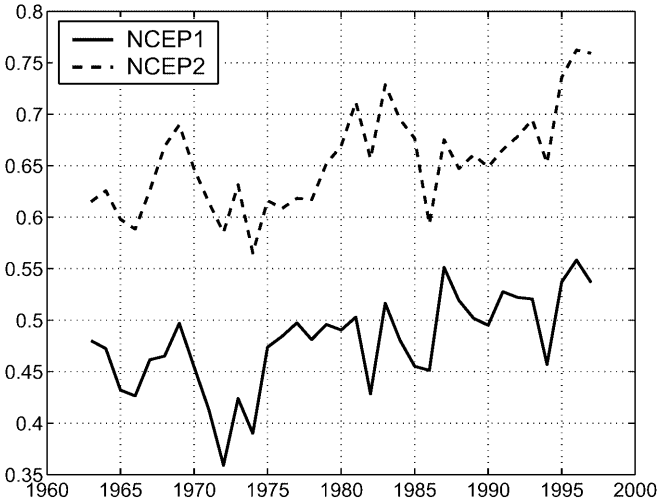

Fig. 14 Time series of meridional heat transport (in PW) in experiments NCEPl and NCEP2, averaged between 39°N and 53°N

has any consequences for the MHT variability. Figure 14 shows time series of MHT, averaged between 39°N and 53°N, i.e. over the region where the mean MHT exhibits a different behaviour. The correlation between the two curves is 0.75, suggesting that the heat flux retroaction term acts almost as a constant offset and that it influences the interannual and decadal MHT fluctuations only by slightly modifying their amplitudes (for completeness we note that after linearly detrending the two signals their correlation is 0.58). An inspection of time series of the zonally integrated heat-flux retroaction term, integrated over the same latitude range, reveals that its variance is much lower in both experiments than the variance of the net surface heat flux (i.e. the natural fluctuations). A correlation of 0.74 underlines that the retroaction term has a similar temporal characteristic in both experiments, although its absolute values are considerably different. Once again, this shows that the different overflow regimes lead to changes in the mean circulation, but that this does not alter the modelled reaction to atmospheric forcing fluctuations in a stand-alone ocean model. It would be interesting to analyze comparable experiments with a coupled ocean–atmosphere model, where a change in the oceanic current patterns could influence the evolution of the atmospheric circulation.

5 Discussion and conclusions

A non-eddy-resolving model of the Atlantic Ocean has been used to study the variability of the large-scale North Atlantic circulation under different circulation regimes characterized by different representations of the overflows from the GIN sea into the subpolar basin. The reference experiment shows both long-term trends and interannual fluctuations that are related to NAO variability. With the NAO changing from a mostly negative phase during the 1960s to high values in the 1990s, the MOC (measured by the meridional overturning stream function) increases in strength. On shorter time scales, both instantaneous and delayed responses to fluctuations in the atmospheric forcing can be found. Our simulated circulation variability is very similar to the results of Eden and Willebrand (2001). In agreement with their explanation, the overturning in our simulation reacts instantaneously to changes in the surface Ekman transport and shows a delayed response to fluctuations in the convective activity in the Labrador Sea.

By modifying the widths and depths of the shallow passages in the Greenland–Iceland–Scotland ridge, the transport of dense water masses across the ridge has been changed in experiments NCEP2 and NCEP3. This causes changes in the mean circulation state of our simulation: the volume transport of overflow water almost doubles, and the maximum density directly south of the sills increases by 0.05–0.08 σ_0 units. In agreement with the results of Döscher and Redler (1997), who found a stronger meridional overturning in their experiments with a higher northern restoring density, the overturning is approximately 2 Sv higher in our experiments NCEP2 and NCEP3 in comparison with NCEPl. Roberts and Wood (1997) report similar changes as a response to modifications of the model bathymetry, although the overturning increase is even larger in their experiments.The increase of the overturning stream function in NCEP2 and NCEP3 is not as large as the corresponding increase of the overflow transport, since a part of the overflow waters recirculates in the subpolar gyre.

The comparison of the deep flow fields in our simulations revealed the possibility that – depending on the relative strength of DSOW and ISOW overflow – two modes of deep circulation might exist in the subpolar North Atlantic that have not been reported by previous authors. The first mode is characterized by a weak

transport of dense waters between Iceland and Scotland and an NADW export from the subpolar gyre to the south that occurs exclusively in the DWBC that follows the continental slope off the Grand Banks of Newfoundland. In the second mode, the ISOW overflow is comparable to or larger than the transport through Denmark Strait, and NADW is transported southward in two current branches on either side of the Mid-Atlantic Ridge. Recent observational data suggest that such export pathways in the basin interior might exist in addition to the DWBC (Bower et al. 2002; Fine et al. 2002), but the details of the simulation of NADW pathways necessitate further study with models of higher resolution or more sophisticated representations of the bottom topography. We note that Biastoch et al. (2003) simulate strong variations of the relative mean strength of DSOW and ISOW transports in response to modifications of the large-scale wind forcing over the subpolar North Atlantic. Although the absolute ISOW transport in our experiment NCEP2 is likely to be overestimated, their study might support the existence of two different paths for the overflow water masses depending on the strength of the wind field.

In contrast to the ISOW transport, the outflow of DSOW exhibits considerable interannual variability in NCEP2 and NCEP3. This is similar to an experiment with a global ocean model described by Nilsen et al. (2003) and to a run with a 1/6° model of the Atlantic with an open boundary at 70°N (B. Barnier, personal communication). Nilsen et al. (2003) find a correlation between both the inflow of surface water over the Iceland–Scotland ridge and the outflow of DSOW on one hand and a NAO-like atmospheric pressure pattern on the other hand, which is in agreement with our explanation for the enhanced DSOW variability (cf. Sect. 4.2). It remains unclear, however, why the ISOW outflow does not show significant temporal fluctuations. Since we are not aware of observational data that would support this partitioning of overflow variability, we cannot judge whether it is real or a model artefact, and we therefore do not speculate about possible reasons here. Dedicated experiments with models of sufficiently high resolution would be required to study the relation between atmospherically induced variability and fluctuations of the overflow branches.

As a result of the modifications of the stratification in the eastern basin of the subpolar North Atlantic, the cyclonic circulation becomes more intensive in this region and the subpolar gyre reaches further to the southeast in experiments NCEP2 and NCEP3. Along with this, the path of the NAC undergoes significant changes. These modifications of the horizontal circulation are in accordance with the regional model studies by Penduff et al. (2000) and Redler and Böning (1997). One effect of this is changes in the T/S properties of subpolar water masses: because of the misrepresentation of the NAC path in the western basin, the retroaction term of the surface heat-flux forcing creates an artificial heat flux into the ocean in the Newfoundland Basin and the region of the Northwest Corner, where in reality the warm surface waters advected from the south by the NAC should be present. This is one of the reasons why the mean temperature of LSW is 0.5 °C higher in the experiments with modified sills.

The oceanic reaction to interannual forcing fluctuations, however, is not influenced by different overflows. Both the sensitivity of local processes like convection in the Labrador Sea and of the large-scale overturning circulation to year-to-year changes in the atmospheric fluxes remain the same. The conclusion of Döscher and Redler (1997) that the influence of decadal atmospheric forcing variability on the strength of the meridional overturning could be overestimated in the absence of realistic overflows might be true for very large changes of the overflow properties as in their experiment C0-1. Fluctuations of the atmospheric forcing as observed during the past decades, however, have a significant influence on the meridional overturning and on the MHT in our simulations regardless of the strength of the northern overflows. Note that both the model setup and the atmospheric forcing used by Döscher and Redler (1997) differed from our study: for example, their experiments did not take into account changes in the wind forcing, and the northern boundary in their model consisted of a restoring zone at 65°N, thereby excluding an explicit representation of the overflows. This implies that dedicated comparison studies would be necessary in order to investigate the influence of extreme overflow conditions. Future experiments should also take into account possible effects of higher model resolution or improved parametrizations (such as a bottom boundary layer scheme).

The volume transport across the Greenland–Iceland–Scotland ridge is too high in comparison with observations in both NCEP2 and NCEP3. The more realistic value of the maximum overflow density in the subpolar North Atlantic is thus achieved at the cost of unrealistic changes in other elements of the circulation. A BBL parameterization could be a better way to represent the T/S properties without changes in the volume transport. Dengg et al. (1999) report only slight changes in the strength of the overturning cell when the BBL is turned on in their experiments, whereas Döscher and Beckmann (2000) observe an increase of almost 50% as a response to the BBL implementation. One should note that they use an additional temperature restoring in Denmark Strait in order to create a DSOW with realistic T/S properties. As far as the variability of the large-scale circulation is concerned, Eden (1999) found the same results as we in NCEP-forced experiments with and without a BBL parameterization: the mean strength is slightly changed, but the response to interannual forcing fluctuations remains the same, which, together with our simulations, gives further justification to "hindcasting" studies of oceanic variability with stand-alone ocean models (such as the ones used by Häkkinen l999, Eden and Willebrand 2001 or Gulev et al. 2003).

We note the limitations of our study because of the fixed restoring zone at the northern boundary: here climatological T/S values have been used to represent the influence of the Arctic Ocean. Therefore, no conclusions can be drawn from our experiments concerning a possible influence of interannual changes in the T/S properties (as a result of a modified sea-ice export through Pram Strait, for example) or the volume transport of water masses originating north of 70°N on fluctuations of the North Atlantic circulation. Furthermore, we cannot judge the relative importance of these changes compared to the influence of the atmospheric forcing over the North Atlantic.

Like several previous studies, our experiments highlight the critical role of the overflow representation for the large-scale circulation in coarse-resolution ocean models. In coupled climate models, the sensitivity of the ocean component to topographic details might have important implications for the simulation of ocean–atmosphere interaction. As long as coarse-resolution ocean models have to be used in coupled climate simulations, an appropriate representation of the overflows is an essential ingredient for a realistic simulation. The use of BBL schemes like the one proposed by Beckmann and Döscher (1997) can help to maintain the high densities of overflow water masses, but a locally refined model grid or a nesting technique could be promising tools to simulate the overflows and their boundary current character dynamically correctly.

Acknowledgements We acknowledge financial support from the German Academic Exchange Service (DAAD) through HSP III, which made a stay of J.-O. Beismann at LEGI possible, during which a considerable part of this work was done. This work was part of the CLIPPER project, funded by grants from CNRS, IFREMER, CMO and CNES. Model simulations were run at the IDRIS computer center in Orsay, France. We are grateful to Jean-Marc Molines, who managed the CLIPPER models. Comments by two anonymous reviewers helped to improve the manuscript.

Appendix: Formulation of the atmospheric forcing

The motivation of the relaxation term in the formulation of the atmospheric forcing is to account for the air–sea coupling (or feedback) and for possible biases in air–sea flux estimates. A variety of approaches are proposed in the literature (Barnier et al. 1995; Seager et al. 1995; Large et al. 1997; Barnier 1998; Eden and Willebrand 2001). However, only few studies have compared these formulations (e.g. Paiva and Chassignet 2001), and more studies are required to provide objective arguments to prefer one parameterization to another, according to scientific objectives.

We use here the surface forcing formulation proposed by Barnier (1998). The solar radiation is treated separately. Its penetration into the upper ocean is formulated as a depth-dependent heating rate which follows the absorption law of clear seawater. The non-solar surface heat flux which is applied at a time t as the surface boundary condition of the model temperature equation, $Q_{NS}(t)$, has two parts. It is formulated as:

$$Q_{NS}(t) = Q'_{NS}(t) - \frac{\partial Q}{\partial T}[SST(t) - T_S(t)]. \quad (1)$$

The first term on the right-hand side of Eq. (l), $Q'_{NS}(t)$, is the non-solar surface heat flux (i.e. the algebraic sum of the longwave, latent and sensible heat fluxes) from the NCEP/NCAR reanalysis at this time. The second term on the right-hand side Eq. (l) is the restoring term that we mentioned in the description of the forcing in Section 2. This term is expressed as the sensitivity (or derivative) of the net heat flux with respect to the sea-surface temperature. We use the spatially varying climatological monthly mean values of $\partial Q/\partial T$ calculated by Barnier et al. (1995). $SST(t)$ is the NCEP/NCAR SST at this time and $T_s(t)$ is the surface temperature calculated by the model, also at this time. The restoring term can be seen as a feedback of the ocean on the surface fluxes, since it modifies the surface heat flux according to the evolution of the model SST.

The equation of salinity is driven by a virtual salt flux as described in Barnier (1998), proportional to a freshwater flux, $(E-P)(t)$ which reflects the water budget at time t:

$$(E-P)(t) = [E(t) - P(t)] + \frac{\Delta z}{\tau}\left[\frac{SSS - S_S(t)}{S_S(t)}\right], \quad (2)$$

where $E(t)$ is evaporation, $P(t)$ is precipitation, both from the NCEP/NCAR reanalysis, $S(t)$ is the surface salinity calculated by the model, τ is a relaxation time and Δz is the thickness of the first model layer. SSS is equivalent to an observed sea-surface salinity at the same time t. However, since the sea-surface salinity is poorly observed at monthly time scales, values of SSS used in Eq. (2) are seasonal estimates from the climatology of Reynaud et al. (1998) interpolated at time t. The relaxation time scale τ is the same as for the temperature. Note, however, that unlike for the temperature, there is no physical justification based on any feedback process for the restoring term in salinity. It is used to prevent a strong drift of the model salinity.

The major interest of this forcing formulation is that it allows for prognostic meridional heat and freshwater transports, while preventing a strong drift of the model SST and SSS away from observed values. As a consequence of the formulation of the feedback term used here, the SST and the SSS in our experiments are identified more with forcing functions than with prognostic variables.

References

Barnier B (1998) Forcing the ocean. In: Chassignet E, Verron J (eds) Ocean modeling and parameterization. Kluwer, New York, pp 45–80

Barnier B, Marchesiello P, de Miranda AP, Molines Jm, Coulibaly M (1998) A sigma-coordinate primitive equation model for studying the circulation in the South Atlantic, part I.

Model configuration with error estimates. Deep-Sea Res I 45: 543–572
Barnier B, Siefridt L, Marchesiello P (1995) Thermal forcing for a global ocean-circulation model using a 3-year climatology of ECMWF analyses. J Mar Syst 6: 363–380
Beckmann A, Döscher R (1997) A method for improved representation of dense water spreading over topography in geopotential-coordinate models. J Phys Oceanogr 27: 581–591
Beismann J-O, Redler R (2003) Model simulations of CFC uptake in North Atlantic Deep Water: effects of parameterizations and grid resolution. J Geophys Res 108: 3159. doi: 10.1029/2001JC001253
Biastoch A, Käse RH, Stammer DB (2003) The sensitivity of the Greenland–Scotland Ridge overflow to forcing changes. J Phys Oceanogr 33: 2307–2319
Blanke B, Delecluse P (1993) Variability of the tropical Atlantic Ocean simulated by a general circulation model with two different mixed-layer physics. J Phys Oceanogr 23: 1363–1388
Böning CW, Bryan FO (1996) Large-scale transport processes in high-resolution models. In: Krauss W (ed) The warm water sphere of the North Atlantic Ocean. Borntraeger, Berlin, pp 91–128
Böning CW, Dieterich C, Barnier B, Jia Y (2001) Seasonal cycle of meridional heat transport in the subtropical North Atlantic: a model intercomparison in relation to observations near 25°N. Prog Oceanogr 48: 231–253
Bower AS, Le Cann B, Rossby T, Zenk W, Gould J, Speer K, Richardson PL, Prater MD, Zhang H-M (2002) Directly measured mid-depth circulation in the northeastern North Atlantic Ocean. Nature 419: 603–607
Dengg J, Böning C, Ernst U, Redler R, Beckmann A (1999) Effects of an improved model representation of overflow water on the subpolar North Atlantic. Int WOCE Newslett 10–15
Dickson RR, Lazier J, Meincke J, Rhines P, Swift J (1996) Long-term coordinated changes in the convective activity of the North Atlantic. Progr Oceanogr 38: 241–295
Dickson B, Meincke J, Vassie J, Jungclaus J, Østerhus S (1999) Possible predictability in overflow from the Denmark Strait. Nature 397: 243–246
Döscher R, Beckmann A (2000) Effects of a bottom boundary layer parameterization in a coarse-resolution model of the North Atlantic Ocean. J Atmos Ocean Technol 17: 698–707
Döscher R, Redler R (1997) The relative importance of northern overflow and subpolar deep convection for the North Atlantic thermohaline circulation. J Phys Oceanogr 27: 1894–1902
Eden C (1999) Interannual to interdecadal variability in the North Atlantic Ocean. PhD Thesis, Christian-Albrechts-Universität Kiel, Germany
Eden C, Willebrand J (2001) Mechanism of interannual to decadal variability of the North Atlantic circulation. J Climat l4: 2266–2280
Fine RA, Rhein M, Andrié C (2002) Using a CFC effective age to estimate propagation and storage of climate anomalies in the deep western North Atlantic Ocean. Geophys Res Lett 29: 2227. DOI: 10.1029/2002GL015618
Ganachaud A, Wunsch C (2003) Large-scale ocean heat and freshwater transports during the world ocean circulation experiment. J Climat 16: 696–705
Girton JB, Sanford TB, Käse RH (2001) Synoptic sections of the Denmark Strait overflow. Geophys Res Lett 28: 1619–1622
Gulev SK, Barnier B, Knochell H, Molines J-M, Cottet M (2003) Water mass transformation in the North Atlantic and its impact on the meridional circulation: insights from an ocean model forced by NCEP/NCAR reanalysis fluxes. J Climat l6: 3085–3110
Häkkinen S (1999) Variability of the simulated meridional heat transport in the North Atlantic for the period 1951–1993. J Geophys Res 104: 10991—11007
Hansen B, Østerhus S (2000) North Atlantic-Nordic Seas exchanges. Prog Oceanogr 45: 109–208
Hurrell JW (1995) Decadal trends in the NAO: regional temperatures and precipitation. Science 269: 676–679
Kalnay EMK, Kistler R, Collins W, Deaven D, Gandin L, Iredell M, Saha S, White G, Woolen J, Zhu Y, Chelliah M, Ebisuzaki W, Higgins W, Janowiak J, Mo KC, Ropelewski C, Leetmaa A, Reynolds R, Jenne R (1996) The NCEP/NCAR reanalysis project. Bull Am Meteorol Soc 77: 437–471
Käse RH, Girton JB, Sanford TB (2003) Structure and variability of the Denmark Strait Overflow: model and observations. J Geophys Res 108: 3181, doi: 10.1029/2002JC001548
Krahmann G, Visbeck M, Reverdin G (2001) Formation and propagation of temperature anomalies along the North Atlantic Current. J Phys Oceanogr 3l: 1287–1303
Large WG, Danabasoglu G, Doney SC, McWilliams JC (1997) Sensitivity to surface forcing and boundary layer mixing in a global ocean model: annual mean climatology. J Phys Oceanogr 27: 2418–2447
Lohmann G (1998) The influence of a near-bottom transport parameterization on the sensitivity of the thermohaline circulation. J Phys Oceanogr 28: 2095–2103
Macdonald AM, Wunsch C (1996) An estimate of global ocean circulation and heat fluxes. Nature 382: 436–439
Madec G, Delecluse P, Imbard M, Lévy C (1998) OPA 8.1 ocean general circulation model reference manual. Notes du pôle de modélisation vol 11, Institut Pierre-Simon Laplace (IPSL), France, 91 pp
Madec G, Chartier M, Delecluse P, Crepon M (1991) A three-dimensional numerical study of deep water formation in the northwestern Mediterranean Sea. J Phys Oceanogr 21: 1349–1371
McCartney MS (1992) Recirculating components to the deep boundary current of the northern North Atlantic. Prog Oceanogr 29: 283–383
Nilsen JEØ, Gao Y, Drange H, Furevik T, Bentsen M (2003) Simulated North Atlantic-Nordic Seas water mass exchanges in an isopycnic OGCM. Geophys Res Lett 30, doi:10.1029/2002GL016597
Orlanski I (1976) A simple boundary condition for unbounded hyperbolic flows. J Comput Phys 21: 251–269
Paiva AM, Chassignet EP (2001) The impact of surface flux parameterizations on the modelling of the North Atlantic Ocean. J Phys Oceanogr 31: 1860–1879
Penduff T, Barnier B, de Verdière AC (2000) Self-adapting open boundaries for a sigma coordinate model of the eastern North Atlantic. J Geophys Res 105: 11279–11297
Peterson RG, Stramma L (l991) Upper-level circulation in the South Atlantic Ocean. Progr Oceanogr 26: 1–73
Redler R, Böning CW (1997) Effect of the overflows on the circulation in the subpolar North Atlantic: a regional model study. J Geophys Res 102: 18529–18552
Reynaud T, LeGrand P, Mercier H, Barnier B (1998) A new analysis of hydrographic data in the Atlantic and its application to an inverse modelling study. Int WOCE Newslett 32: 29–31
Roberts MJ, Wood RA (1997) Topographic sensitivity studies with a Bryan–Cox-type ocean model. J Phys Oceanogr 27: 823–836
Rodwell MJ, Rowell DP, Folland CK (1999) Oceanic forcing of the wintertime North Atlantic oscillation and European climate. Nature 398: 320–323
Sarkisyan AS, Ivanov VE (1971) Joint effect of baroclinicity and bottom relief as an important factor in the dynamics of sea currents. Akad Nauk Atmosph Oceanic Phys 7: 173–188
Schott F, Lee TN, Zantopp R (1988) Variability of structure and transport of the Florida Current in the period range of days to seasonal. J Phys Oceanogr 18: 1209–1230
Seager R, Blumenthal M, Kushnir Y (1995) An advective atmospheric mixed layer model for ocean modelling purposes: global simulation of surface heat fluxes. J Phys Oceanogr 8: 1951–1964
Smith WHF, Sandwell DT (1997) Global seafloor topography from satellite altimetry and ship depth soundings. Science 277: 1956–1962
Talley LD (2003) Shallow, intermediate, and deep overturning components of the global heat budget. J Phys Oceanogr 33: 530–560

Tréguier A-M, Reynaud T, Pichevin T, Barnier B, Molines J-M, de Miranda AP, Messager C, Beismann J-O, Madec G, Grima N, Imbard M, Le Provost C (1999) The CLIPPER project: high-resolution modelling of the Atlantic. Int WOCE Newslett 36: 3–5

Tréguier AM, Barnier B, de Miranda AP, Molines JM, Grima N, Imbard M, Madec G, Messager C, Reynaud T, Michel S (2001) An eddy-permitting model of the Atlantic circulation: evaluating open boundary conditions. J Geophys Res 106: 22115–22130

Willebrand J, Barnier B, Böning C, Dieterich C, Killworth PD, Le Provost C, Jia Y, Molines J-M, New AL (2001) Circulation characteristics in three eddy-permitting models of the North Atlantic. Progr Oceanogr 48: 123–161

Yashayaev I (2001) Computer atlas of the northwest Atlantic. CD-ROM, Bedford Institute of Oceanography